Journal of Materials Processing Technology 153–154 (2004) 1019–1025

Journal of Materials Processing Technology

www.elsevier.com/locate/jmatprotec

# Determination of work material flow stress and friction for FEA of machining using orthogonal cutting tests

Tuğrul Özel*, Erol Zeren

*Department of Industrial and Systems Engineering, Rutgers, The State University of New Jersey, Piscataway, NJ 08854, USA*

**Abstract**

Finite element analysis based techniques are available to simulate cutting processes and offer several advantages including prediction of tool forces, distribution of stresses and temperatures, estimation of tool wear and residual stresses on machined surfaces, optimization of cutting tool geometry and cutting conditions. However, work material flow stress and friction characteristics at cutting regimes are not always available. This paper utilizes a metal cutting model developed by Oxley and presents an improved methodology to characterize work material flow stress and friction at primary and secondary deformation zones around the cutting edge by utilizing orthogonal cutting tests. In this paper, Johnson–Cook (JC) constitutive work flow stress model is used to characterize work flow stress in deformation zones. The friction model is based on estimation of the normal stress distribution over the rake face. The stress distribution over the tool rake face can either directly be entered in FEA software or used in determining a coefficient of the friction at the tool-chip interface. The methodology is practical and estimates the unknowns of both the work material constitutive model and the friction model over the rake face.


*Keywords:* Flow stress; Friction; Orthogonal cutting; Constitutive models

## 1. Introduction

There has been a considerable amount of research devoted to develop analytical, mechanistic and numerical models in order to simulate metal cutting processes. Especially, numerical models are highly essential in predicting chip formation, computing forces, distributions of strain, strain rate, temperatures and stresses on the cutting edge and the chip and the machined work surface [9]. The premise of the numerical models is to be able to lead further predictions in machinability, tool wear, tool failure, and surface integrity on the machined surfaces. Success and reliability of numerical models are heavily dependent upon work material flow stress models in function of strain, strain rate and temperatures, as well as friction parameters between the tool and work material interfaces [8].

In material removal processes using geometrically defined cutting edges, work material goes severe deformations and shearing at very high deformation rates and temperatures. Work material flow stress determined through tensile and/or compression tests may not be valid to represent deformation behavior in the ranges of strain, strain rate and temperature observed during especially high-speed machining, a popular operation to increase productivity. In addition, friction between work material and cutting tool surface plays a significant role in predicted or simulated force, stress and temperature distributions. It has been repeatedly overstressed that a good understanding of metal cutting mechanics and reliable work material flow stress data and friction characteristics between the work material and the cutting tool edges must be generated for high-speed cutting conditions [9].

## 2. Constitutive models for work material flow stress

The flow stress or instantaneous yield strength at which work material starts to plastically deform or flow is mostly influenced by temperature, strain, strain rate, and other factors. Accurate and reliable flow stress models are considered highly necessary to represent work material constitutive behavior under high-speed cutting conditions especially for a (new) material. Unfortunately sound theoretical models based on atomic level material behavior are far from being materialized as reported by Jaspers and Dautzenberg [12]. Therefore, semi-empirical constitutive models are widely utilized. The constitutive model proposed by Johnson and Cook [4] describes the flow stress of a material with the product of strain, strain rate and temperature effects that

* Corresponding author. Tel.: +1 732 455 1099; fax: +1 732 455 5467.
*E-mail address:* ozel@rci.rutgers.edu (T. Özel).

0924-0136/$ – see front matter © 2004 Elsevier B.V. All rights reserved.
doi:10.1016/j.jmatprotec.2004.04.162

are individually determined as given in Eq. (1).

$$\bar{\sigma} = [A + B(\bar{\varepsilon})^n]\left[1 + C\ln\left(\frac{\dot{\bar{\varepsilon}}}{\dot{\bar{\varepsilon}}_0}\right)\right]\left[1 - \left(\frac{T - T_{\text{room}}}{T_{\text{melt}} - T_{\text{room}}}\right)^m\right] \quad (1)$$

In the Johnson–Cook (JC) model, the parameter $A$ is in fact the initial yield strength of the material at room temperature and a strain rate of $1\,s^{-1}$ and $\bar{\varepsilon}$ represents the plastic equivalent strain. The strain rate $\dot{\bar{\varepsilon}}$ is normalized with a reference strain rate $\dot{\bar{\varepsilon}}_0$. Temperature term in JC model reduces the flow stress to zero at the melting temperature of the work material, leaving the constitutive model with no temperature effect. In general, the parameters $A$, $B$, $C$, $n$ and $m$ of the model are fitted to the data obtained by several material tests conducted at low strains and strain rates and at room temperature as well as split Hopkinson pressure bar (SHPB) tests at strain rates up to $1000\,s^{-1}$ and at temperatures up to 600 °C [8]. JC model provides good fit for strain-hardening behavior of metals and it is numerically robust and can easily be used in finite element simulation models [12]. An alternative constitutive model for metals is derived from dislocation-mechanics theory with a crystal structure distinction by Zerilli and Armstrong (ZA) [5].

Many researchers used JC model as constitutive equation for high strain rate, high temperatures deformation behavior of metals. Hamann et al. [6] investigated the effect of metallurgical treatments after deoxidation of free machining steels on the machinability by conducting orthogonal cutting tests, a SHPB test, and numerical simulations of the cutting process. They used a reversed method to identify parameters for JC constitutive model for two low carbon free cutting steels, namely S300 and S300 Si and two low-alloyed structural free machining steels, 42CD4 U and 42CD4 Ca. Lee and Lin [7] fitted SHPB test results in to JC model to study high temperature deformation behavior of Ti6Al4V, a titanium alloy. Meyer and Kleponis [10] also studied high strain rate behavior of Ti6Al4V and fitted their experiments into JC model. Both research groups also discussed advantages and disadvantages of using JC model as constitutive equation for Ti6A4V. Jaspers and Dautzenberg [12] have concluded that strain rate and temperature dramatically influence the flow stress of metals, steel AISI 1045 and aluminum AA 6082-T6, according to measurements with SHPB tests. Firstly, they used JC and ZA constitutive models to find parameters in the equations, and then compared results to the measurements. To calculate parameters, they did not prefer to use least square estimator method because of its difficulty. Instead the parameters are investigated by leaving only one parameter unconstrained, whereas the others are kept constant, and consequently all parameters are found for both models (Table 1).

## 3. Prior research in determination of flow stress models from orthogonal cutting test

Late Oxley developed an analytical model to predict cutting forces and average temperatures and stresses in the primary and secondary deformation zones by using (a) flow stress data of the work material as a function of strain and velocity-modified temperature which couples strain rate to temperature, (b) thermal properties of the work material, (c) tool geometry and (d) cutting conditions. Oxley also utilized slip-line field analysis to model chip formation in metal cutting. He applied his theory to cutting of low carbon steel and obtained flow stress and friction data by empirically fitting the results of the orthogonal cutting tests [3].

Several researchers have used Oxley's predictive machining approach, in order to obtain work flow stress data [11–14]. Recently, Shatla et al. [11] modified JC flow stress model and used Oxley's parallel sided thin shear zone theory and empirically determined parameters of the modified JC model by applying orthogonal high-speed slot milling experimentation technique developed by Özel and Altan [9]. In an attempt to utilize orthogonal cutting tests in determining flow stress data, Shatla et al. presented some findings for the modified JC model for tool steels AISI P20 and AISI H13, and aluminum, Al 2007. Tounsi et al. [13] stated a re-evaluated methodology related to analytical modeling of orthogonal metal cutting—continuous chip

Table 1
Parameters of JC constitutive model for some metals

| Material | Reference | $A$ | $B$ | $n$ | $C$ | $m$ | Test |
|---|---|---|---|---|---|---|---|
| Ti6Al4V | Lee and Lin (1998) | 782.7 | 498.4 | 0.28 | 0.028 | 1.0 | SHPB |
| AISI 1045 | Jaspers and Dautzenberg (2002) | 553.1 | 600.8 | 0.234 | 0.0134 | 1 | SHPB |
| AA 6082-T6 | Jaspers and Dautzenberg (2002) | 428.5 | 327.7 | 1.008 | 0.00747 | 1.31 | SHPB |
| 35NCD16 | Taunsi et al. (2002) | 848 | 474 | 0.288 | 0.0230 | 0.540 | OCT |
| INOX316L | Taunsi et al. (2002) | 514 | 514 | 0.508 | 0.0417 | 0.533 | OCT |
| 42CD4 U | Taunsi et al. (2002) | 589 | 755 | 0.198 | 0.0149 | 0.800 | OCT |
| S300 | Taunsi et al. (2002) | 245 | 608 | 0.35 | 0.0836 | 0.144 | OCT |
| S300 | Hamann et al. (1996) | 240 | 622 | 0.35 | 0.09 | 0.25 | SHPB |
| S300 Si | Hamann et al. (1996) | 227 | 722 | 0.40 | 0.123 | 0.20 | SHPB |
| 42CD4 U | Hamann et al. (1996) | 598 | 768 | 0.209 | 0.0137 | 0.807 | SHPB |
| 42CD4 Ca | Hamann et al. (1996) | 560 | 762 | 0.255 | 0.0192 | 0.660 | SHPB |
| Ti6Al4V | Meyer and Kleponis (2001) | 862.5 | 331.2 | 0.34 | 0.0120 | 0.8 | SHPB |

formation—process to identify variables of JC constitutive model. They applied least-square approximation techniques to obtain those variables. Primary shear zone is assumed having a constant thickness, and according to experiments and data that found from literature, its value is approximated by one-half of the uncut chip thickness. Along with data published by Hamann et al. [6] for 42CD4 U, and S300, orthogonal cutting experiments are undertaken for stainless steel 316L and 35NCD16 to verify the effectiveness of proposed methodology. However, they neither presented an adequate formulation for the friction at the chip-tool interface in their model, nor attempted to determine friction parameters.

The research focus of this paper is to determine the values of the workpiece material flow stress parameters represents the excessive strain rates and temperatures during machining process. To calculate these values, results of the orthogonal cutting experiments including measured values for machining forces, chip thickness, and tool-chip contact length are utilized. Specifically, based on orthogonal cutting tests, the parameters of the JC model are calculated in the primary deformation zone using Oxley's slip-line field analysis in reverse [3]. The same experimental data is used in determining the frictional parameters on the tool rake face. An experimentally determined slip-line field proposed by Tay et al. [2] of the secondary deformation zone is used to determine the shearing stress $k_{int}$ in the sticking region and coefficient of friction $\mu$ in the sliding region.

## 4. Analytical model for orthogonal metal cutting

The plastic deformation for the formation of a continuous chip when machining a ductile material is illustrated in Fig. 1. It is commonly recognized that the primary plastic deformation takes place in a finite-sized deformation zone. The work material begins to deform when it enters the primary deformation zone from lower boundary CD, and it continues to deform as the material streamlines follow smooth curves until it passes the upper boundary EF. There is also a secondary plastic deformation zone adjacent to the tool-chip interface that is caused by the intense contact pressure and frictional force. After exiting from the primary deformation zone, some material experiences further plastic deformation in the secondary deformation zone. Using the quick-stop method to experimentally measure the flow field, Oxley [3] proposed a slip-line field similar to the one shown in Fig. 1. The slip-line field and the corresponding hodograph indicated that the strain rate in the primary deformation zone increases with cutting speed and has a maximum value at plane AB. Based on this experimental observations, he proposed the empirical relation in Eq. (2) for the average value of the shear strain rate along AB. The velocity along the shear plane is also given by Eq. (3).

$$\dot{\gamma}_{AB} = C_0 \frac{V_S}{l_{AB}} \tag{2}$$

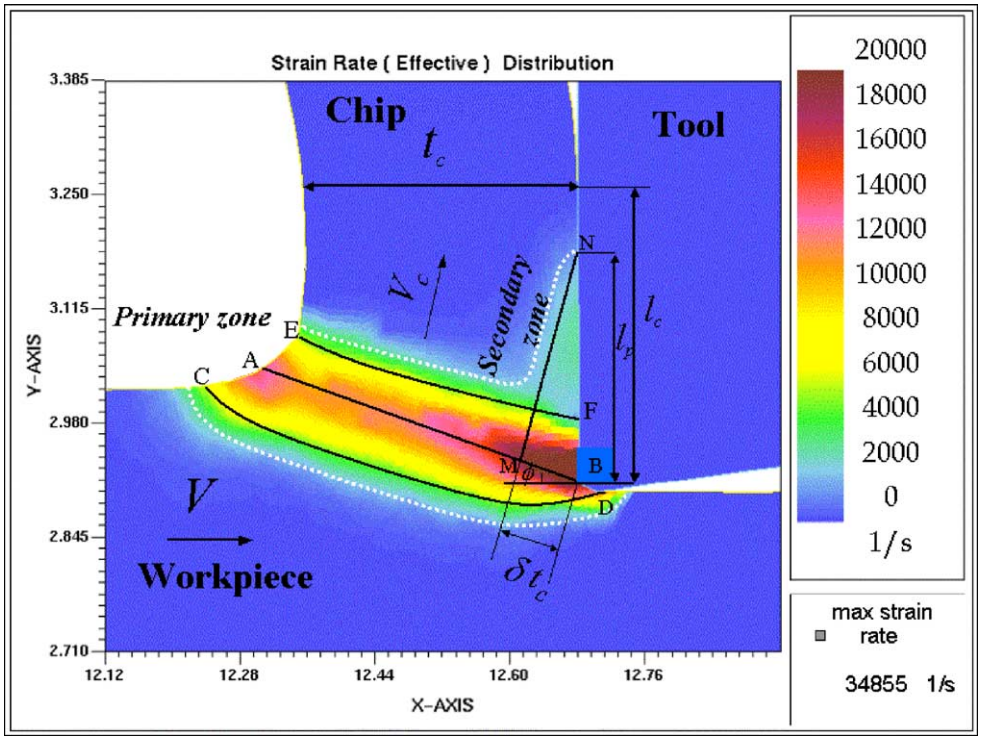


Fig. 1. Deformation zones in orthogonal cutting as illustrated on FEM simulation of chip formation in AISI P20 steel and carbide tool (after Özel and Altan [9]).

$$V_S = \frac{V\cos\alpha}{\cos(\phi-\alpha)} \tag{3}$$

where $V$ is the cutting speed, $\alpha$ the rake angle, $V_S$ the shear velocity and $\phi$ is the shear angle. Given by Eq. (2), $l_{AB}$ is the length of AB, and $C_0$ is the material constant. The shear angle $\phi$ can be estimated from Eq. (4).

$$\phi = \tan^{-1}\left(\frac{(t_u/t_c)\cos\alpha}{1-(t_u/t_c)\sin\alpha}\right) \tag{4}$$

where $t_u$ is the undeformed chip thickness, and $t_c$ is the measured chip thickness. Oxley also found that $C_0 = 5.9$ for the mild steel used in their experiments [3]. Although the strain rate is slightly higher in the vicinity of the tool cutting edge, its value remains relatively constant over the majority of plane AB. Therefore, Eq. (2) represents a reasonable approximation of strain rate for plane AB. The shear strain occurring in the primary deformation zone, and therefore, corresponds to the average shear strain in the primary deformation zone.

$$\gamma_{AB} = \frac{\cos\alpha}{2\sin\phi\cos(\phi-\alpha)} \tag{5}$$

In the primary zone, the shear stress stays same on plane AB, and the average value of shear stress at AB is given by Eq. (6).

$$k_{AB} = \frac{F_S\sin\phi}{t_u w} \tag{6}$$

where $w$ is the width of the chip, and the shear force $F_S$ is calculated from the measured cutting force $F_C$ and feed force $F_T$, as shown in Eq. (7).

$$F_S = F_C\cos\phi - F_T\sin\phi \tag{7}$$

Due to the difficulties associated with routinely measuring meaningful machining temperatures, developing mathematical models for machining temperature has been widely used as an attractive alternative. In Oxley's model [3], the average shear plane temperature $T_{AB}$ is given by Eq. (8)

$$T_{AB} = T_0 + \frac{(1-\beta)F_S\cos\alpha}{\rho S t_u w\cos(\phi-\alpha)} \tag{8}$$

where $T_0$ is the initial workpiece temperature, $\rho$ the density, $S$ the specific heat value of the work material, $\beta$ the fraction of the energy generated in the primary zone that enters in the workpiece and determined [3].

$$\begin{aligned}\beta &= 0.5 - 0.35\log(R_T\tan\phi) \quad \text{for } 0.04 \le R_T\tan\phi \le 10.0\\ \beta &= 0.3 - 0.15\log(R_T\tan\phi) \quad \text{for } R_T\tan\phi > 10.0\end{aligned} \tag{9}$$

with $R_T$ a non-dimensional thermal number given where $K$ is the thermal conductivity of the work material by

$$R_T = \frac{\rho S V t_u}{K} \tag{10}$$

The average temperature of the primary deformation zone can be estimated using Eq. (8). The average shear strain rate, shear strain, and shear stress in the primary deformation zone are given by Eqs. (2), (5) and (6), respectively. Using the Von Mises criterion, they can be related to the equivalent stress, strain, and strain rate using Eq. (11).

$$\bar{\sigma}_{AB} = \sqrt{3}k_{AB}, \qquad \bar{\varepsilon}_{AB} = \frac{\gamma_{AB}}{\sqrt{3}}, \qquad \dot{\bar{\varepsilon}}_{AB} = \frac{\dot{\gamma}_{AB}}{\sqrt{3}} \tag{11}$$

In order to determine the parameters of the JC constitutive model, a set of orthogonal cutting experiments is performed to measure the forces $F_C$ and $F_T$ in various cutting conditions and later values of $\bar{\varepsilon}_{AB}$, $\dot{\bar{\varepsilon}}_{AB}$, $\bar{\sigma}_{AB}$, and $T_{AB}$ are computed.

Using inverse solution of Oxley's model to find the desired parameters $A$, $B$, $C$, $m$, $n$ is in fact quite challenging due to the non-linearity in the JC constitutive model. Other researchers proposed various techniques to address this problem. Shatla et al. [11] reported that their algorithm is vulnerable finding local convergence as the unrealistic combinations of JC parameters as the solution.

In this work, the parameters of JC model are determined by using non-linear regression algorithm based on the Gauss–Newton algorithm with Levenberg–Marquardt modifications for global convergence. The only unknown value at this point is $C_0$, which is given by Eq. (12).

$$C_0 = \frac{(p_A - p_B)(A\varepsilon_{AB}^{-n} + B)}{2Bnk_{AB}} \tag{12}$$

$p_A$ and $p_B$ are the hydrostatic stresses at points A and B, respectively, which can be determined from measured machining forces and stress state at point A as shown by Oxley [3]. $C_0$ is solved in an iterative procedure and parameters of the JC constitutive model are computed. Therefore, the flow stress parameters can be directly used in the finite element simulations of metal cutting.

## 5. Analytical model for friction at the tool-chip interface

The normal stress is greatest at the tool tip and gradually decreases to zero at the point where the chip separates from the rake face [3]. The frictional shearing stress distribution is more complicated. Over the portion of the tool-chip contact area near the cutting edge, sticking friction occurs, and the frictional shearing stress is equal to $k_{int}$ [1]. Over the remainder of the tool-chip contact area, sliding friction occurs, and the frictional shearing stress can be calculated using the coefficient of friction $\mu$. This section describes a methodology to determine the shearing stress in the sticking region and the coefficient of friction in the sliding region, based on the measured machining forces, $F_C$ and $F_T$, and the measured tool-chip interface contact length $l_C$. The normal stress distribution on the tool rake face can be described by Eq. (13).

$$\sigma_N(x) = \sigma_{N_{max}}\left[1 - \left(\frac{x}{l_C}\right)^a\right] \tag{13}$$

where $x$ is the distance from the cutting edge, and $a$ is an empirical coefficient that must be calculated. Integrating the

normal stress along the entire tool-chip contact length yields the relation in Eq. (14).

$$F_N = \int_0^{l_C} w\sigma_N(x)\,dx = \int_0^{l_C} w\sigma_{N_{max}}\left[1-\left(\frac{x}{l_C}\right)^a\right]dx \quad (14)$$

$F_N$ is the normal force on the tool rake rake face determined from Eq. (15)

$$F_N = F_C\cos\alpha - F_T\sin\alpha \quad (15)$$

Oxley [3] showed that $\sigma_{N_{max}}$ can be estimated by analyzing the hydrostatic stress along AB, yielding Eq. (16).

$$\sigma_{N_{max}} = k_{AB}\left(1+\frac{\pi}{2}-2\alpha-2\frac{BnC_0}{A\varepsilon_{AB}^{-n}+B}\right) \quad (16)$$

Combining Eqs. (14)–(16), it can be shown that the exponential coefficient $a$ is given by Eq. (17).

$$a = \frac{F_N}{wl_Ck_{AB}(1+(\pi/2)-2\alpha-2(BnC_0/A\varepsilon_{AB}^{-n}+B))-F_N} \quad (17)$$

Normal stress distribution over the rake face is fully defined and the coefficient of friction can be obtained, once the values of the parameters $\sigma_{N_{max}}$ and $a$ are found. The shear stress distribution on the tool rake face illustrated in Fig. 1 can be represented in two distinct regions (a) in the sticking region with $\tau_f(x) = k_{int}$ and when $\mu\sigma_N(x) \geq k_{int}$, (b) in the sliding region with $\tau_f(x) = \mu\sigma_N(x)$, $0 < x \leq l_P$ and when $\mu\sigma_N(x) < k_{int}$, $l_P < x \leq l_C$. Here $k_{int}$ is the shear flow stress of the material in the secondary zone and it is related to the frictional force between the chip and the tool, $F_F$ as given in Eq. (18).

$$F_F = \int_0^{l_P} wk_{int}\,dx + \int_{l_P}^{l_C} w\mu\sigma_N(x)\,dx \quad (18)$$

The relation between the average coefficient of friction in the sliding region $\mu$ and $k_{int}$is:

$$\mu = \frac{k_{int}}{\sigma_N(l_P)} \quad (19)$$

Combining Eqs. (18) and (19) leads to the expression for $k_{int}$ in Eq. (20)

$$k_{int} = \frac{F_F}{\left(wl_P + \frac{w}{\sigma_N(l_P)}\int_{l_P}^{l_C}\sigma_N(x)\,dx\right)} \quad (20)$$

The frictional force component $F_F$ is given by Eq. (21).

$$F_F = F_C\sin\alpha + F_T\cos\alpha \quad (21)$$

As shown in Fig. 1, shape of the secondary plastic zone in the sticking region can be assumed triangular according to Tay et al. [2]. On the rake face point N is located at the interface between the sticking and sliding regions. Line MN is a II slip-line that is assumed to be straight. Similar to the approach proposed by Oxley [3] can be taken to analyze hydrostatic stresses along MN, and to compute the length of sticking region, $l_P$ along with using Eq. (22).

$$l_P = \frac{\delta t_C}{\sin(\phi-\alpha)} \quad (22)$$

where $\delta t_C$ is the maximum thickness of the secondary zone as shown in Fig. 1. $\delta$ is another parameters yet to be determined iteratively. According to Oxley [3], in the secondary zone, the average shear strain rate and shear strain are considered constant and can be estimated from Eqs. (23) and (24).

$$\dot{\gamma}_{int} = \frac{V_C}{\delta t_C} \quad (23)$$

$$\gamma_{int} = \frac{l_C}{\delta t_2} \quad (24)$$

The average tool-chip interface temperature is the average temperature at the primary zone and the maximum temperature rise in the chip as given in Eq. (25).

$$T_{int} = T_{AB} + \Delta T_M \quad (25)$$

$\Delta T_M$ can be calculated once the thickness of the tool-chip interface $\delta t_C$, and the tool-chip contact length $l_C$ are found.

$$\log\frac{\Delta T_M}{\Delta T_C} = 0.06 - 0.195\,\delta\left(\frac{R_T t_c}{l_C}\right)^{1/2} + 0.5\log\left(\frac{R_T t_c}{l_C}\right) \quad (26)$$

The shear flow stress, shear strain rate, shear strain, and temperature for the secondary zone are given by Eqs. (20) and (23)–(25), respectively. The only unknown in the solution process is the value of $\delta$ based on the minimum work criterion proposed by Oxley [3]. As derived in Appendix A, the difference between hydrostatic stresses at points M and N ($p_M$ and $p_N$, respectively) is given in Eq. (27).

$$p_M - p_N = k_{int}\left[2(\phi-\alpha) + \left(\frac{(Bn\varepsilon_{int}^n)/\gamma_{int}}{A+B\varepsilon_{int}^n}\right)\frac{l_p\sin\phi}{\delta\sin(\phi-\alpha)}\right] \quad (27)$$

As shown in Fig. 1, point M is on line AB, and $p$ changes proportionally along AB as $p_B < p_A$ remains and the hydrostatic stress at point M can be given by Eq. (28).

$$p_M = p_B + \frac{\delta t_C}{l_{AB}}(p_A - p_B) \quad (28)$$

The hydrostatic stress at point N is equal to the normal stress at $l_P$.

$$p_N = \sigma_N(l_P) \quad (29)$$

The only unknown in Eqs. (27)–(29), $\delta$ can be solved in an iterative procedure and the coefficient of friction in the sliding region, $\mu$, can be determined as part of the entire determination of the flow stress and frictional parameters using orthogonal cutting test.

## 6. Conclusions and future work

The goal of this work is to present a methodology in order to determine work material flow stress and friction properties for use in finite element simulations of metal cutting processes. For this purpose, a work material constitutive model developed by Johnson and Cook is used as the work flow stress model. The friction models consist of three parameters (a) normal and frictional stress distributions, (b) length of the plastic region in the secondary zone, (c) coefficient of friction in the sliding region. The parameters of the JC constitutive model and frictional parameters can be computed in an iteration scheme by utilizing an inverse solution of Oxley's machining theory and forces measured in orthogonal cutting tests for various cutting conditions. This methodology will be applied to characterize flow stress for AISI P20 mold steel and AISI H13 tool steel and the friction parameters at the tool-chip interface by using the orthogonal cutting tests. Then, the flow stress model will be compared with the other models determined for the same materials.

## Appendix A

The slip-line field analysis reveals the equilibrium equations as Eq. (A.1) on the AB with a I slip-line and as Eq. (A.2) on the MN with a II slip-line.

$$\frac{\partial p}{\partial s_2} + 2k\frac{\partial \psi}{\partial s_1} - \frac{\partial k}{\partial s_2} = 0 \tag{A.1}$$

$$\frac{\partial p}{\partial s_2} - 2k\frac{\partial \psi}{\partial s_2} - \frac{\partial k}{\partial s_1} = 0 \tag{A.2}$$

In the above equations, $p$ and $k$ are the hydrostatic stress and shear flow stress of the work material, $\Psi$ the angular rotation, and $s_1$ and $s_2$ are distances measured along I and II lines, respectively. Both lines AB and MN are assumed straight along slip-lines I and II, respectively. On line AB the equilibrium equation becomes

$$\frac{p_A - p_B}{l_{AB}} = \frac{dk}{ds_2} \tag{A.3}$$

Right side of the above equation can be written as

$$\frac{dk}{ds_2} = \frac{dk}{d\gamma}\frac{d\gamma}{dt}\frac{dt}{ds_2} \tag{A.4}$$

Recall that shear flow stress is a function of strain, strain-rate and temperature constituted by Johnson–Cook model

$$\frac{dk}{d\gamma} = k_{AB}\frac{(Bn/\gamma_{AB})(\gamma_{AB}/\sqrt{3})^n}{A + B(\gamma_{AB}/\sqrt{3})^n} \tag{A.5}$$

$$\frac{d\gamma}{dt} = \frac{C_0 V\cos\alpha}{l_{AB}\cos(\phi - \alpha)} \tag{A.6}$$

$$\frac{dt}{ds_2} = \frac{1}{V\sin\phi} \tag{A.7}$$

Substituting Eqs. (A.4)–(A.7) into Eq. (A.3) yields Eq. (A.8)

$$p_A - p_B = \frac{2k_{AB}BnC_0}{A\varepsilon_{AB}{}^{-n} + B} \tag{A.8}$$

Similarly, the equilibrium equation along line MN that is given with Eq. (A.2) becomes Eq. (A.9) when it is assume to be straight, the strain-rate and temperature are considered unchanged in the secondary zone.

$$\frac{p_M - p_N}{l_{MN}} - 2\frac{k_{int}(\phi - \alpha)}{l_{MN}} = \frac{dk}{ds_1} \tag{A.9}$$

$$\frac{dk}{ds_1} = \frac{dk}{d\gamma}\frac{d\gamma}{dt}\frac{dt}{ds_1} \tag{A.10}$$

$$\frac{dk}{d\gamma} = k_{int}\frac{(Bn/\gamma_{int})(\gamma_{int}/\sqrt{3})^n}{A + B(\gamma_{int}/\sqrt{3})^n} \tag{A.11}$$

$$\frac{d\gamma}{dt} = \frac{V\sin\phi}{\delta t_C\cos(\phi - \alpha)} \tag{A.12}$$

$$\frac{dt}{ds_1} = \frac{1}{V\sin(\phi - \alpha)} \tag{A.13}$$

Substituting Eqs. (A.10)–(A.13) into Eq. (A.9) yields Eq. (A.14)

$$p_M - p_N + 2k_{int}(\phi - \alpha) = k_{int}\left(\frac{Bn/\gamma_{int}}{A\varepsilon_{int}^{-n} + B}\right)\frac{\sin\phi}{\sin^2(\phi - \alpha)}. \tag{A.14}$$

## References


[1] N.N. Zorev, Inter-Relationship Between Shear Processes Occurring Along Tool Face and Shear Plane in Metal Cutting, International Research in Production Engineering, ASME, New York, (1963), 42–49.

[2] A.O. Tay, M.G. Stevenson, M.G.G. de Vahl Davis, Using the finite element method to determine temperature distributions in orthogonal machining, Proc. Inst. Mech. Eng. 188 (1974) 627–638.

[3] P.L.B. Oxley, Mechanics of Machining, an Analytical Approach to Assessing Machinability, Ellis Horwood Limited, 1989.

[4] G.R. Johnson, W.H. Cook, A constitutive model and data for metals subjected to large strains, high strain rates and high temperatures, in: Proceedings of the 7th International Symposium on Ballistics, The Hague, The Netherlands, (1983), 541–547.

[5] F.J. Zerilli, R.W. Armstrong, Dislocation-mechanics-based constitutive relations for material dynamics calculations, J. Appl. Phys. 61 (5) (1987) 1816–1825.

[6] J.C. Hamann, V. Grolleau, F. Le Maitre, Machinability improvement of steels at high cutting speeds – study of tool/work material interaction, Ann. CIRP 45 (1996) 87–92.

[7] W.S. Lee, C.F. Lin, High-temperature deformation behavior of Ti6Al4V alloy evaluated by high strain-rate compression tests, J. Mater. Process. Technol. 75 (1998) 127–136.

[8] T.H.C. Childs, Material property needs in modeling metal machining, in: Proceedings of the CIRP International Workshop on Modeling

of Machining Operations, Atlanta, Georgia, USA, 19 May 1998, 193–202.
[9] T. Özel, T. Altan, Determination of workpiece flow stress and friction at the chip-tool contact for high-speed cutting, Int. J. Machine Tools Manuf. 40 (1) (2000) 133–152.
[10] H.W. Meyer Jr., D.S. Kleponis, Modeling the high strain rate behavior of titanium undergoing ballistic impact and penetration, Int. J. Impact Eng. 26 (2001) 509–521.
[11] M. Shatla, C. Kerk, T. Altan, Process modeling in machining. Part I: Determination of flow stress data, Int. J. Machine Tools Manuf. 41 (2001) 1511–1534.
[12] S.P.F. C Jaspers, J.H. Dautzenberg, Material behavior in conditions similar to metal cutting: flow stress in the primary shear zone, J. Mater. Process. Technol. 122 (2002) 322–330.
[13] N. Tounsi, J. Vincenti, A. Otho, M.A. Elbestawi, From the basic mechanics of orthogonal metal cutting toward the identification of the constitutive equation, Int. J. Machine Tools Manuf. 42 (2002) 1373–1383.
[14] Y. Huang, S.Y. Liang, Cutting forces modeling considering the effect of tool thermal property-application to CBN hard turning, Int. J. Machine Tools Manuf. 43 (2003) 307–315.